Nuclear Instruments and Methods in Physics Research B 488 (2021) 23–29

Contents lists available at ScienceDirect

Nuclear Inst. and Methods in Physics Research, B

journal homepage: www.elsevier.com/locate/nimb

Effect of pulsed electron beam treatment on microstructure and functional properties of Al-5.4Si-1.3Cu alloy

Dmitrii Zaguliaev [a,b], Yurii Ivanov [c], Sergey Konovalov [a,d,*,1], Vitalii Shlyarov [b], Damir Yakupov [b], Andrey Leonov [c]

[a] Wenzhou University Institute of Laser and Optoelectronic Intelligent Manufacturing, Wenzhou 325024, China
[b] Siberian State Industrial University, Novokuznetsk 654007, Russia
[c] Institute of High Current Electronics of the Siberian Branch of the RAS, Tomsk 634055, Russia
[d] Samara National Research University, Samara 443086, Russia

ARTICLE INFO

Keywords:
Al-5.4Si-1.3Cu alloy
Pulsed electron beam
Functional properties
Wear resistance
Microhardness
Microstructure

ABSTRACT

The effect of pulsed electron beam treatment (density of energy 10, 30, and 50 J/cm^2 and pulse times 50 and 200 μs) on the microstructure and functional properties of the Al-5.4Si-1.3Cu alloy is traced via exploring its microhardness, wear resistance and microstructure. The research pointed out the wear resistance of the alloy irradiated with pulsed electron beam to be 197% higher than the same characteristic of the untreated material. A maximal microhardness increase was recorded for following electron beam treatment parameters: 30 J/cm^2, 200 μs and 50 J/cm^2, 50 μs; the values of microhardness were as high as 860 MPa and 950 MPa, respectively. Key factors responsible for better wear resistance and higher microhardness in the samples treated with a pulsed electron beam were suggested to be silicon and intermetallic compounds, dissolving in the molten surface, a cellular nano-dimensional structure, resulting from rapid solidification, and nano-dimensional particles of silicon and multi-element compounds.

1. Introduction

Aluminum, to be more precise, an alloy on its base was synthesized by a Danish physicist Hans Christian Ersted in 1825; but its factory production and use were first mentioned in 1886. To date, aluminum alloys represent the next broadly used metallic constructional materials after iron and steel. These alloys are applied in aircraft, space, motor vehicle, navy and gun industries due to their unique properties, such as low density, high specific strength and sufficient corrosion resistance [1–5]. Each aluminum-based alloy irrespectively to its grade is distinguished with a quite broad application scope. In particular, the Al-5.4Si-1.3Cu alloy under study is a material used in machine elements and mechanisms of civil aircraft and motor vehicle engineering, supports and fixtures of furniture production and in the manufacture of various components for household appliances, etc. [6,7].

Recently, machine parts are manufactured of aluminum using traditional techniques, e.g. casting, forging, stamping, and powder metallurgy [8,9]. Despite a broad use, the manufacture and consumption of these goods have been experiencing certain problems. For instance, a low speed of cooling in casting is the reason for rough microstructure and numerous defects, e.g. displacement damages, shrinkage porosity, slag inclusions and segregation of elements in cast alloys, as a consequence mechanical properties of machine parts degrade [10–14]. Industrial conglomerates introducing stronger standards for the structure and operation characteristics of machine parts made of aluminum and its alloys make the situation even more difficult. To illustrate, materials with a lattice or cell structure, the production of which represents a complex and science intensive issue, are needed to satisfy technical requirements for high heat conductivity, a light weight, and high specific strength of heat protection systems in airspace vehicle engines. In the integrated manufacturing process of complex structure elements it is possible to reduce a time and a number of tools while producing and assembling small and middle-sized components, to decrease their weight, make less concentrated stresses arising in welding or mounting machine parts [15–19]. The principal aim of future research and development is suggested to be the advancement of

* Corresponding author at: Wenzhou University Institute of Laser and Optoelectronic Intelligent Manufacturing, Ocean Science and Technology Innovation Park, No. 19 Binhai 3rd Road, Yongxing Street, Longwan District, Wenzhou, Zhejiang 325024, China.

E-mail addresses: zagulyaev_dv@physics.sibsiu (D. Zaguliaev), ksv@ssau.ru (S. Konovalov).

[1] Samara National Research University, 34, Moskovskoye Shosse, Samara 443086, Russia.

https://doi.org/10.1016/j.nimb.2020.12.004
Received 6 November 2020; Received in revised form 30 November 2020; Accepted 10 December 2020
Available online 18 December 2020

technologies to produce alloys with specified properties. Nevertheless certain attempts have been already made to modify materials through surface treatment with concentrated energy flows [20–23]. Laser and electron beam treatment are important surface processing methods. Laser processing has a positive effect on Al and its alloys, slows down a propagation rate of the fatigue crack growth [22], enhances corrosion resistance [24], changes the surface morphology; furthermore, microstructural transformations improve the welding of aluminum products [25] and their mechanical properties [26,27].

Besides laser processing, electron beam treatment represents one of the promising surface treatment techniques intended to advance physical and technical characteristics of a product and form a unique structure of metals and alloys [28–30]. Electron beam melting technologies are known to be a surface processing method of Al-Si alloys and a self-sufficient production process of these alloys [31]. The study demonstrated an ultrafine grained structure with better functional properties to evolve in electron beam melting. The electron beam treatment of Al-Si alloys led to the surface remelting and changed the element and phase composition as a consequence. Several works [32–34] reported on close to the total dissolution of primary Si crystals in the modified layer in electron beam melting and disclosed transformations of the Al crystal lattice parameter for the oversaturated solid solution of aluminum was formed in the molten layer. Tribological tests made it possible to claim the wear resistance of processed alloys to be considerably better than this characteristic of untreated Al-Si compounds [31–37]. A number of works have examined the effect of various treatment processes on the structuring and behavior of mechanical properties in Al-5Si alloys. Several studies paid particular attention to the role of laser in surface processing or for the total remelting of Al-5Si alloys [38,39]. The researchers argued that laser processing improves the functional properties, refines the microstructure and changes the element and phase composition. The explorations we present in this paper are unique for the alloy with the given chemical composition. This study aimed to analyze the behavior of functional properties (wear resistance and microhardness) of Al-5.4Si-1.3Cu alloy surface irradiated with a pulsed electron beam in different modes and reveal why they changed. The outcomes of the research may be of crucial importance to the machine building industry as a post-processing procedure to advance technical characteristics.

2. Material and methods of research

For the purpose of research, we used the Al-5.4Si-1.3Cu alloy; its chemical composition determined relying on the X-ray analysis data is given in Fig. 1a. When manufacturing, the alloy was poured into moulds in liquid form under the gravitation force and made solidify at an ambient temperature. Prepared samples were squares (dimensions – 15 $\times$ 15 $\times$ 5 mm^3) (Fig. 1b).

The irradiation of samples with an intensive electron beam was performed using the “SOLO” laboratory unit [40]. It encompasses a pulsed electron source based on a plasma cathode with grid stabilization of a plasma edge, a power supply of the electron source, a vacuum processing chamber with an inspection opening and a two-dimensional manipulator table, where a plasma source and samples to be irradiated are placed, as well as systems to control and test the parameters of an electron source and a beam [41].

An electron beam was directed along the normal line to a sample side with dimensions of 15 $\times$ 15 mm^2, and a beam diameter was set to cover a sample surface totally (Fig. 1d).

The electron beam parameters were as follows: energy of accelerated electrons 17 keV, energy density of the electron beam (10, 30, 50) J/cm^2, pulse time (50 and 200) μs, number of pulses 3, pulse frequency 0.3 s^{-1}; residual gas (argon) pressure in the processing chamber $2{\cdot}10^{-2}$ Pa.

For selecting maximal processing parameters (50 J/cm^2, 200 μs) it was important to melt the surface layer without boiling the material affected with an electron beam.

The wear resistance of the material was examined relying on the wear parameter (k), a reciprocal of wear resistance, using a TRIBOtester

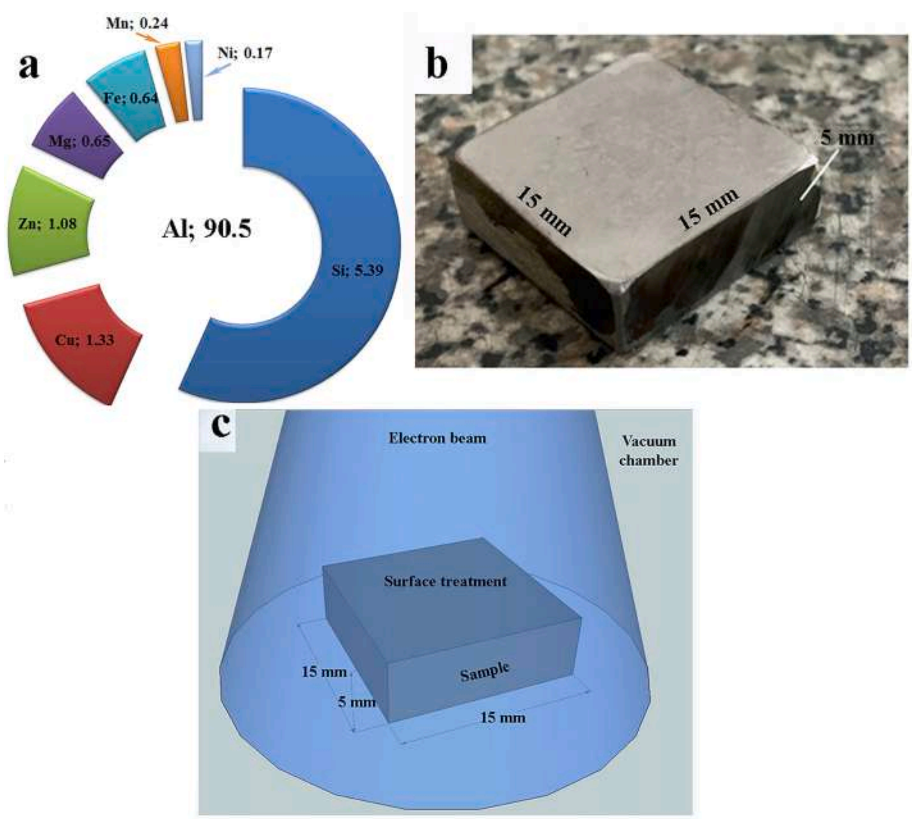

Fig. 1. X-ray analysis data of the material under study (a), geometry of samples (b), a sample oriented to an electron beam (c).

in the Pin-On-Disc scheme. The tests were carried out in dry friction conditions for the parameters: normal loading – 2 N; rotation speed of a sample – 25 mm/s, distance recorded – 100 m; track radius – 2 mm; counterbody – a hard BK7alloy ball with a diameter of 6 mm.

To determine hardness we measured microhardness of the irradiated surface using the Vickers method and following the internationally accepted standard ISO 6507: 2005; an indenter was loaded by 1 N (a microhardness measuring device HVS-1000). The time of loading was set 10 s, and the unloading took 5 s (an average microhardness value was detected with respect to 10 impressions made at least on 3 samples in each mode).

The structure and its components in the material surface were investigated using the methods of scanning electron microscopy (SEM) with Philips SEM-515 equipped with a micro-analyzer EDAX ECON IV, transmission electron microscopy (TEM) in the diffraction mode and scanning transmission electron microscopy (STEM) in a scanning mode with JEM 2100F, JEOL.

The methods of STEM and TEM complement each other, and their combination within one study provides the comprehensive understanding of the material structure because STEM is intended to analyze the structure of a material surface and TEM is developed to explore the structure of a material volume.

The foils to explore a structure-phase state of the material by transmission electron microscopy in the diffraction mode were prepared via ion thinning (Ion Slicer EM-09100IS) of plates. Plates with the 100 μm thickness were cut out of a sample using the electrical discharge process. The mode of cutting was selected to avoid unnecessary deformation; therefore a structure of samples remained unaffected. In each mode we examined minimum 5 samples. Further we present the most typical microphotographs to show the material structure.

3. Results

Fig. 2 displays the tribological test findings and data on microhardness of Al-5.4Si-1.3Cu alloy samples irradiated with an intensive electron beam (red and blue bars). From the data it is apparent the wear parameter drops given the electron beam energy density increases when irradiating with a pulse time of 200 μs and demonstrates a trend to saturation (Fig. 2, red bars). Once the pulse time of electron beam processing is 50 μs (Fig. 2, blue bars), the wear resistance of the alloy is more sophisticated. In this case wear resistance decreases insignificantly for the beam energy density of 30 J/cm^2 and rises if irradiated with the energy density of 50 J/cm^2. Given that the alloy is treated with the 30 J/cm^2 electron beam, micropores are formed in the surface because of the material shrinkage in rapid crystallization conditions, the wear parameter shows a slightly increasing tendency, worsening the wear resistance, as a consequence. However, this shortcoming can be eliminated via increasing the time of surface processing and the beam energy density. A maximal increase of wear resistance ($k = 0.37 \cdot 10^{-3}$ mm^3/N·m) is 197% revealed for the treatment parameters: 50 J/cm^2 200 μs.

While analyzing the data on the microhardness behavior, some conclusions are formulated. Once the pulse time is set 50 μs (a solid line), the microhardness in the surface layer goes up together with the growing energy density of an electron beam, attaining its maximum of 950 MPa for the beam energy density of 50 J/cm^2; this value is 83% higher than the microhardness of the untreated material. Given that the pulse time is 200 μs (a dashed line), the microhardness of the surface is maximal (860 MPa) for the beam energy density of 30 J/cm^2 exceeding the reference value by 65%. It is noteworthy that an increasing value of the beam energy density up to 50 J/cm^2 makes microhardness somehow decrease; principal alloying elements melt and evaporate enormously from the treated surface in this processing mode. The research highlighted the outcomes of electron beam treatment connected with the Si percentage: it is ~3.9 mass% for the beam energy density 50 J/cm^2 and a pulse time of 200 μs, whereas it is ~4.1 mass% for the beam energy density 30 J/cm^2. Therefore, an assumption is made a varying percentage of main alloying elements is the reason less strengthening phases are formed, as a consequence, microhardness decreases. Conversely, values of microhardness in all processing conditions are far higher than this parameter of the untreated material.

Comparing wear parameter data and microhardness values, their correlation is suggested, i.e. the rising electron beam energy density is associated with the decreasing wear parameter (as a result of better wear resistance) and increasing microhardness. Both facts present the evidence surface layers of the material get reinforced.

Therefore, an analysis of wear resistance vs. energy density and pulse time of the electron beam established 50 J/cm^2, 200 μs were the most effective parameters to perform electron beam treatment. The assessment of microhardness revealed the most efficient way of treatment to be in conditions: 50 J/cm^2 and 50 μs.

To find out factors influencing strength properties of the surface, the microstructure was explored using scanning and transmission electron

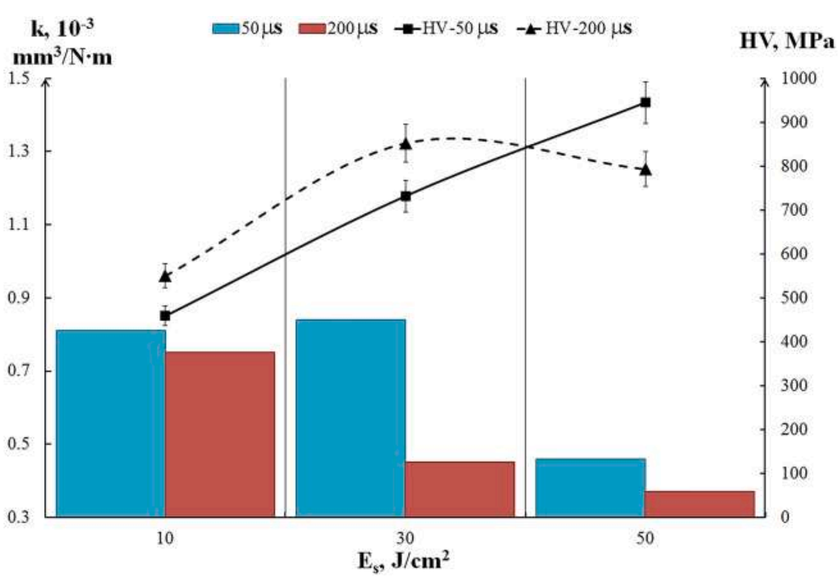

Fig. 2. Wear parameter k and microhardness HV vs. energy density of an electron beam (10, 30 50 J/cm^2) and pulse time (50 and 200 μs). k and HV of as cast alloy are $1.1 \cdot 10^{-3}$ mm^3/N·m and 520 MPa, respectively. (For interpretation of the references to color in this figure legend, the reader is referred to the web version of this article.)

microscopy in the identified optimal modes. The structure of the as delivered alloy (Fig. 3) was examined with the aim to trace structural transformations observed while irradiating samples. Addressing to the microstructure presented in Fig. 3a, it is seen the alloy is a polycrystalline aggregate with micropores (black inclusions) and inclusions of intermetallic compounds (white inclusions) with a variety of shapes (needles, globules, and far less frequently, chips) and sizes. In some cases the intermetallic compounds form hieroglyph-like agglomerates (Fig. 3a, b).

An X-ray analysis detected a structure of the alloy was principally made of aluminum-based solid solution grains. The eutectic grains Al-Si (Fig. 3c) were found along the boundaries and in the boundary joints of aluminum grains. The intermetallic compounds represent additional phases of the material under study, one of which is a $Fe_2Al_9Si_2$ phase (Fig. 3b, c).

The aluminum grains vary in a range from 25 μm to 80 μm; the eutectic grains Al-Si are from 11 μm to 26 μm. The longitudinal sizes of the needle-shaped intermetallic compounds are often bigger than sizes of grains (Fig. 3c), probably, they were formed before aluminum grains.

Particles of the intermetallic compounds with any morphology found in the alloy intensify its brittleness when mechanically loaded.

A structure of the sample surface changed once the Al-5.4Si-1.3Cu alloy was irradiated with the intensive pulsed electron beam (50 J/cm^2 50 and 200 μs). Microcracks (Fig. 4a, c) were detected in the structure of the irradiated material surface. In most cases microcracks were observed along the grain boundaries. Zones surrounded by the microcracks are in a range from 280 μm to 380 μm. Microcracks might propagate owing to the tensile stresses evolving in the surface for the material cooled at a high speed from a molten state. A number of microcracks per a surface area unit of the alloy rose insignificantly if we shortened a pulse time (compare Fig. 4a, c). Apparently, it was caused by an increasing speed of cooling when we reduced a pulse time.

Electron beam irradiation of the alloy in optimal conditions brought about the total dissolution of intermetallic compounds in the surface (Fig. 4). The structure of rapidly solidifying cells with dimensions of 500–800 nm developed in a volume of grains (Fig. 4b, d). To get a deep insight into the structure of rapidly solidifying cells, it was researched by the method of transmission electron microscopy in the diffraction mode (STEM and TEM). The thickness of a layer with rapidly solidifying cells was assessed to be from 50 to 70 μm.

An X-ray microanalysis revealed the cells contained an aluminum-based solid solution; a thin layer to separate the crystallization cells contained silicon, copper, and iron atoms (Fig. 5). The element composition of the foil section presented in Fig. 5a, included magnesium (0.85 mass%), silicon (2.83 mass%), manganese (0.25 mass%), iron (0.54 mass%), nickel (0.06 mass%) and copper (4.07 mass%) balanced by aluminum.

Fig. 6 shows a typical cell crystallization structure obtained by TEM methods. The dark-field images were made on the zone shown by a selective diaphragm on the sample of interest (circle in Fig. 6a). Then we switched to the electron diffraction micro-pattern mode and obtained a diffraction pattern for the selected zone of a foil (Fig. 6b).

A dark-field analysis demonstrated the cells were principally made of the aluminum-based solid solution (Fig. 6c). The cells are separated by thin second phase layers with crystallites ranging from 10 to 20 nm (Fig. 6d). The cell formation mechanism was analyzed in details in the study [42].

A diffraction microanalysis pointed out these crystallites represented principally silicon, although particles containing copper, iron and aluminum were also found.

Therefore, one of the reasons for significantly increasing functional properties of the Al-5.4Si-1.3Cu alloy irradiated with the pulsed electron beam (the energy density of 50 J/cm^2) is suggested to be the total dissolution of intermetallic compounds (found in the structure of the as delivered alloy) in the molten layer of aluminum and the subsequent development of a structure with rapidly solidifying cells reinforced by nano-dimensional silicon and multi-element inclusions.

4. Discussion

To sum up, the outcomes of the investigation show that there are two behavior types of hardness and wear resistance, which depend on the electron beam pulse time.

Hardness and wear resistance tend to increase for a relatively short (50 μs) time of electron beam impact. This phenomenon may result from the incomplete dissolution of micron inclusions (needle-shaped inclusions are observed to dissolve partially), which are found in the untreated material and cause its over-brittleness under friction (the initial state). Nano-dimensional second-phase particles forming in the process of the rapid melt solidification reinforce the material and improve its

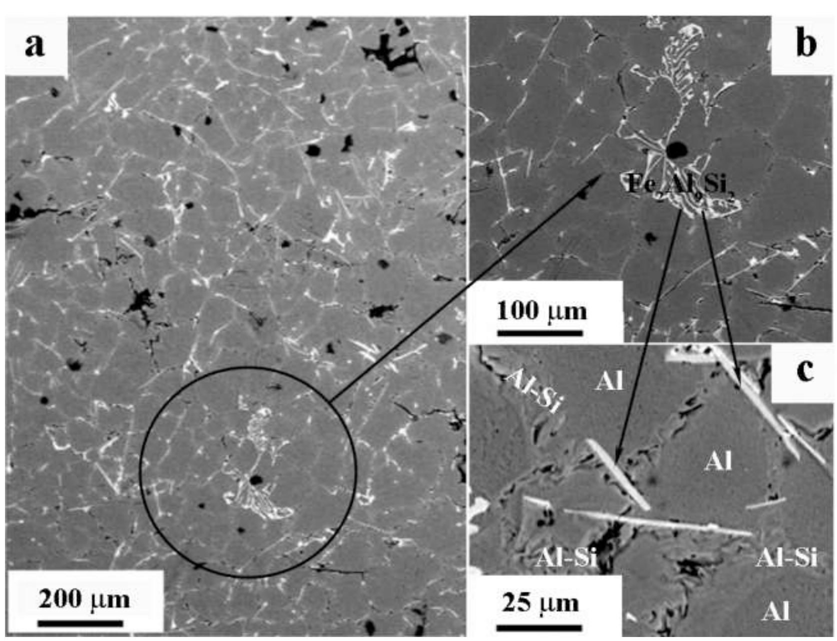

Fig. 3. Structure of destructed surface in the untreated alloy Al-5.4Si-1.3Cu sample (prior the irradiation with a pulsed electron beam).

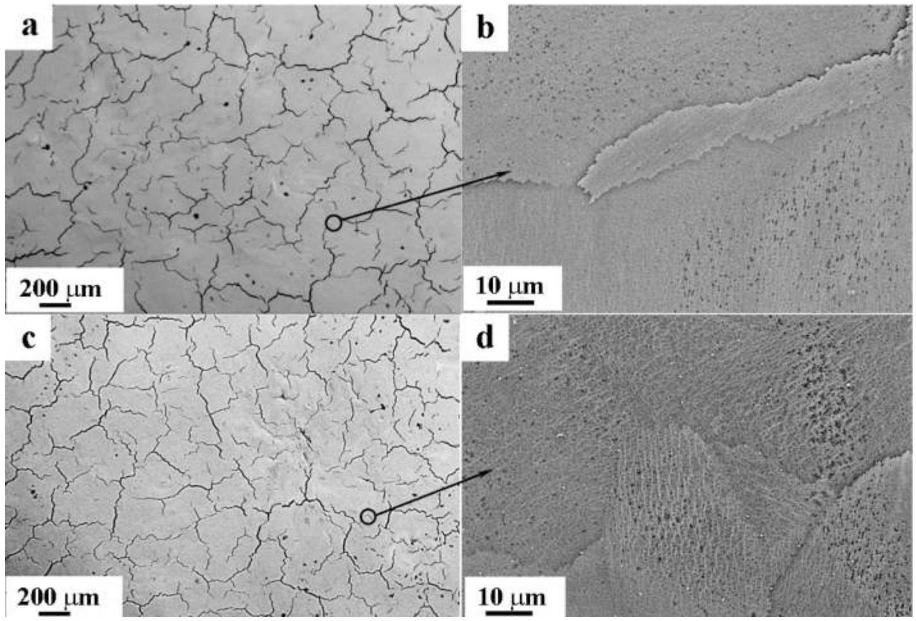

Fig. 4. Surface structure of the alloy Al-5.4Si-1.3Cu irradiated with an electron beam: 50 J/cm^2 200 μs (a, b); 50 J/cm^2 50 μs (c, d). SEM data.

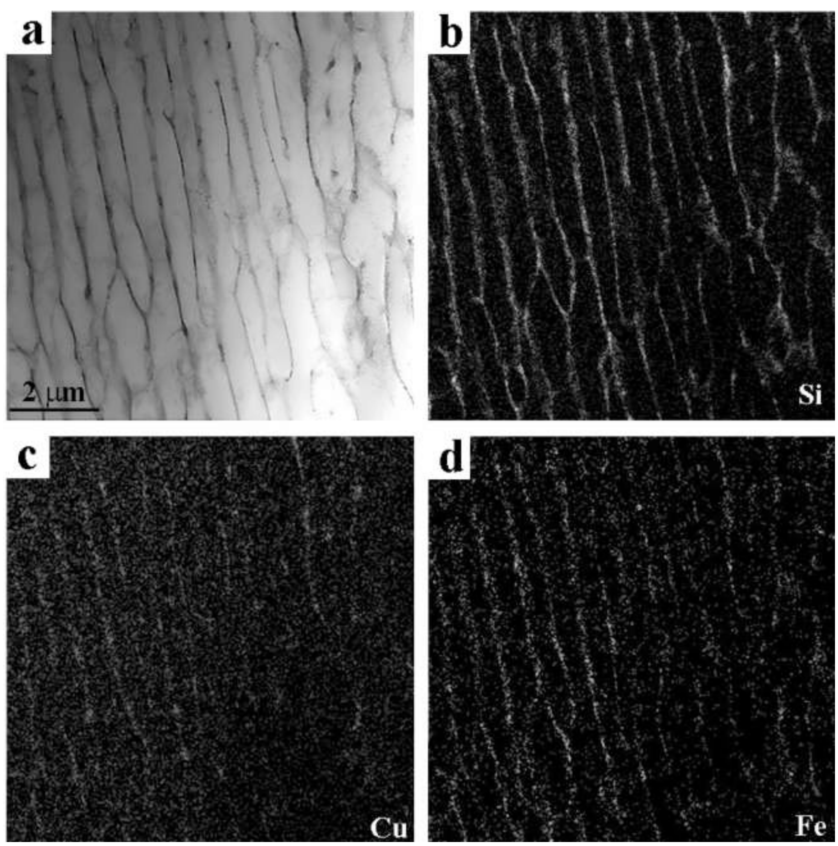

Fig. 5. STEM view of the alloy Al-5.4Si-1.3Cu structure, irradiated with a pulsed electron beam (50 J/cm^2, 50 μs) (a) and a view of this layer obtained in characteristic X-ray radiation of silicon (b), copper (c), and iron (d) atoms. A layer of interest is at a depth of ≈30 μm below the irradiated surface.

hardness.

The hardness and wear resistance of the modified layer in the material demonstrate a simultaneous increase once irradiated for 200 μs (30 J/cm^2). As mentioned above, it may be associated with the incomplete dissolution of needle-shaped micron inclusions existing in the as delivered material and making it extremely brittle under friction. Nano-dimensional second-phase particles formed due to rapidly crystallizing melt make the material stronger and harder.

The electron beam irradiation of the Al-5.4Si-1.3Cu alloy with energy density of 50 J/cm^2 enhances wear resistance and causes a drop of the material microhardness. We conclude a relatively slow energy input (200 μs) furthers the total dissolution of inclusions found in the as

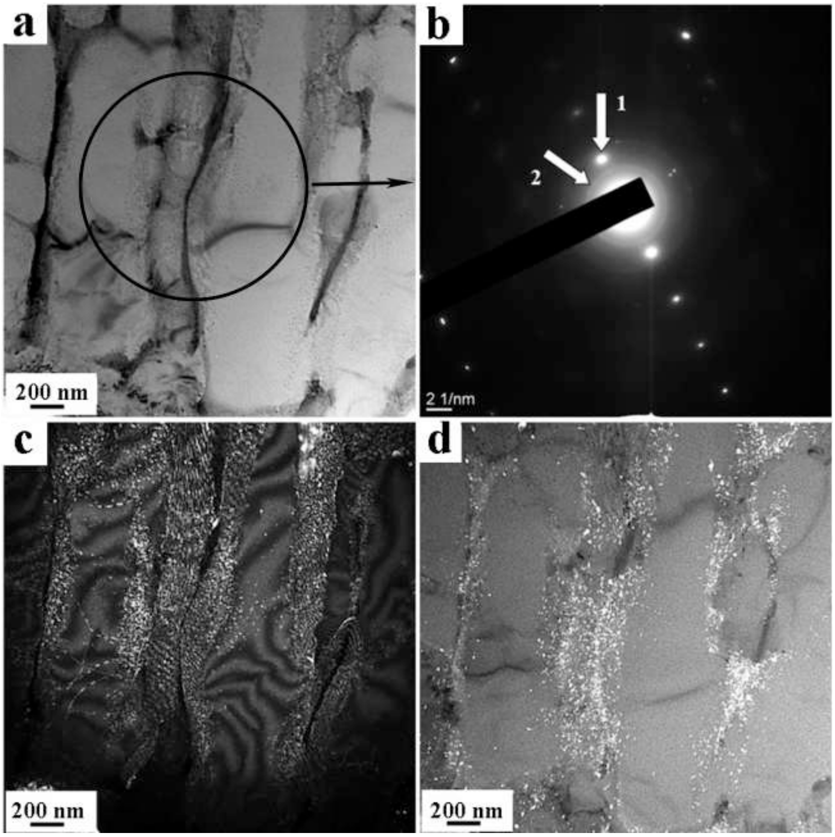

Fig. 6. TEM-view of the alloy Al-5.4Si-1.3Cu structure, irradiated with a pulsed electron beam (50 J/cm^2, 50 μs); a – electron diffraction micro-pattern (bright-field microscopy), selected area electron diffraction is marked with a circle; b – electron diffraction image; c – electron diffraction micro-pattern (dark-field microscopy) obtained in closely-spaced reflexes [1 1 1]Al and [1 0 1]$FeSi_2$ (reflex 1 (b)); d – electron diffraction micro-pattern (dark-field microscopy) obtained in reflex [1 0 0]Si (reflex 2 (b)).

delivered state and they make no contribution to the material reinforcement.

5. Conclusion

To summarize, the irradiation of the Al-5.4Si-1.3Cu alloy with an intensive pulsed electron beam in various modes improved its tribological properties; that is, the wear parameter (a reciprocal of wear resistance) decreased. The wear resistance of the Al-5.4Si-1.3Cu alloy (the irradiation parameters 50 J/cm^2, 200 μs) was detected to be 197% higher than that of the untreated material. A maximal increase in microhardness was 83% as compared with the as delivered alloy and observed for the parameters of the electron beam: 50 J/cm^2 and 50 μs. The electron beam treatment carried out in conditions as follows: the energy density 30 J/cm^2 and a pulse time 50 μs causes the formation of micro-pores on the material surface, resulting in the deteriorating wear resistance of the material. Once the treatment parameters are set 50 J/cm^2 and 200 μs, main alloying elements evaporate form the treated material surface, and a value of microhardness shows a declining trend. Nevertheless, the parameters of interest in all treatment conditions are far higher than the similar characteristics of the untreated alloy. Considering the beam energy density in all treatment modes a conclusion is made that the wear resistance and microhardness of the Al-5.4Si-1.3Cu alloy improve due to the increasing beam energy density. The changing functional properties indicate strengthening of the material surface. The most effective irradiation parameters to further the maximal reinforcement were 50 J/cm^2, 50 and 200 μs.

Using the methods of scanning and transmission electron microscopy, it was revealed a layer of the material with a thickness of 50–70 μm was an irradiation product of the Al-5.4Si-1.3Cu alloy carried out in the most effective modes. No intermetallic compounds making the material brittle were detected in this layer. A structure with rapidly solidifying cells was formed in the volume of grains. This structure reinforced by nano-dimensional silicon and multi-element inclusions varied from 500 to 800 nm. The thin second-phase layer with crystallites of 10–20 nm surrounded cells. Nano-dimensional structures developing in the material surface had a positive effect on its strength characteristics.

To conclude, all structural changes in the alloy of interest observed after the intensive pulsed electron beam irradiation, contributed to the improvement of its functional properties (wear resistance and microhardness).

CRediT authorship contribution statement

Dmitrii Zaguliaev: Conceptualization, Writing - original draft, Writing - review & editing, Formal analysis. **Yurii Ivanov:** Investigation, Writing - original draft, Writing - review & editing. **Sergey Konovalov:** Conceptualization, Writing - original draft, Writing - review & editing. **Vitalii Shlyarov:** Investigation. **Damir Yakupov:** Investigation. **Andrey Leonov:** Investigation, Writing - review & editing.

Declaration of Competing Interest

The authors declare that they have no known competing financial interests or personal relationships that could have appeared to influence the work reported in this paper.

Acknowledgement

The research was granted by Russian Science Foundation (RSF) (project №. 19-79-10059).

References

[1] P. Kaczyński, M. Skwarski, K. Jaśkiewicz, Development of the technology for press-forming of energy-absorbing elements made of 7075 aluminum alloy, J. Manuf. Processes 50 (2020) 676–683, https://doi.org/10.1016/j.jmapro.2020.01.023.

[2] D. Yuan, K. Chen, SongyiChen, L. Zhou, J. Chang, L. Huang, Y. Yi, Enhancing stress corrosion cracking resistance of low Cu-containing Al-Zn-Mg-Cu alloys by slow quench rate, Mater. Des. 164 (2019) 107558, https://doi.org/10.1016/j.matdes.2018.107558.
[3] W. Xu, Y. Luo, W. Zhang, M. Fu, Comparative study on local and global mechanical properties of bobbin tool and conventional friction stir welded 7085-T7452 aluminum thick plate, J. Mater. Sci. Technol. 34 (2018) 173–184, https://doi.org/10.1016/j.jmst.2017.05.015.
[4] R. Bush, M. Kiyota, C. Kiyota, Characterization of a friction stir weld in aluminum alloy 7055 using microhardness, electrical conductivity, and differential scanning calorimetry (DSC), Metall. Mater. Trans. A 47 (2016) 3522–3532, https://doi.org/10.1007/s11661-016-3506-7.
[5] J.C. Williams, E.A. Starke ., Progress in structural materials for aerospace systems. The Golden Jubilee Issue—Selected topics in Materials Science and Engineering: Past, Present and Future, edited by S. Suresh. Acta Mater. 51 (2003) 5775–5799, https://doi.org/10.1016/j.actamat.2003.08.023.
[6] J.C. Benedyk, 3 – Aluminum alloys for lightweight automotive structures, in: P.K.B. T.-M. Mallick Design and Manufacturing for Lightweight Vehicles (Ed.), Woodhead Publ. Ser. Compos. Sci. Eng., Woodhead Publishing, 2010, pp. 79–113, https://doi.org/10.1533/9781845697822.1.79.
[7] D. Brough, H. Jouhara, The aluminium industry: a review on state-of-the-art technologies, environmental impacts and possibilities for waste heat recovery, Int. J. Thermofluids 1–2 (2020) 100007, https://doi.org/10.1016/j.ijft.2019.100007.
[8] S. Li, C. He, J. Fu, J. Xu, G. Xu, Z. Wang, Evolution of microstructure and properties of novel aluminum-lithium alloy with different roll casting process parameters during twin-roll casting, Mater. Charact. 161 (2020) 110145, https://doi.org/10.1016/j.matchar.2020.110145.
[9] C. Hu, T. Ding, H. Ou, Z. Zhao, Effect of tooling surface on friction conditions in cold forging of an aluminum alloy, Tribol. Int. 131 (2019) 353–362, https://doi.org/10.1016/j.triboint.2018.11.002.
[10] H. Ammar, A. Samuel, F. Samuel, Porosity and the fatigue behavior of hypoeutectic and hypereutectic aluminum–silicon casting alloys, Int. J. Fatigue 30 (2008) 1024–1035, https://doi.org/10.1016/j.ijfatigue.2007.08.012.
[11] B. Li, Y. Shen, W. Hu, Casting defects induced fatigue damage in aircraft frames of ZL205A aluminum alloy – a failure analysis, Mater. Des. 32 (2011) 2570–2582, https://doi.org/10.1016/j.matdes.2011.01.039.
[12] X. Liu, Q. Zhu, Y. Kang, Y. Zuo, R. Wang, Z. Li, An investigation of direct-chill cast 2024 aluminum alloy under the influence of high shearing with regards to different shear positions, J. Mater. Process. Technol. 279 (2020) 116547, https://doi.org/10.1016/j.jmatprotec.2019.116547.
[13] I. Serrano-Munoz, J.-Y. Buffiere, C. Verdu, Y. Gaillard, P. Mu, Y. Nadot, Influence of surface and internal casting defects on the fatigue behaviour of A357-T6 cast aluminium alloy, Int. J. Fatigue 82 (2016) 361–370, https://doi.org/10.1016/j.ijfatigue.2015.07.032.
[14] I.Y. Timoshkin, K.V. Nikitin, V.I. Nikitin, V.B. Deev, Influence of treatment of melts by electromagnetic acoustic fields on the structure and properties of alloys of the Al–Si system, Russ. J. Non-ferrous Metals 57 (2016) 419–423, https://doi.org/10.3103/S1067821216050163.
[15] W. Li, K. Yang, S. Yin, X. Yang, Y. Xu, R. Lupoi, Solid-state additive manufacturing and repairing by cold spraying: a review, J. Mater. Sci. Technol. 34 (2018) 440–457, https://doi.org/10.1016/j.jmst.2017.09.015.
[16] R.S. Mishra, Z.Y. Ma, Friction stir welding and processing, Mater. Sci. Eng. R: Rep. 50 (2005) 1–78, https://doi.org/10.1016/j.mser.2005.07.001.
[17] F. Nie, H. Dong, S. Chen, P. Li, L. Wang, Z. Zhao, X. Li, H. Zhang, Microstructure and mechanical properties of pulse MIG welded 6061/A356 aluminum alloy dissimilar butt joints, J. Mater. Sci. Technol. 34 (2018) 551–560, https://doi.org/10.1016/j.jmst.2016.11.004.
[18] Z.L. Ni, F.X. Ye, Ultrasonic spot welding of aluminum alloys: a review, J. Manuf. Processes 35 (2018) 580–594, https://doi.org/10.1016/j.jmapro.2018.09.009.
[19] Y. Zhan, Y. Li, E. Zhang, Y. Ge, C. Liu, Laser ultrasonic technology for residual stress measurement of 7075 aluminum alloy friction stir welding, Appl. Acoust. 145 (2019) 52–59, https://doi.org/10.1016/j.apacoust.2018.09.010.
[20] Z. Lei, Z. Tian, X. Chen, Y. Chen, J. Bi, S. Wu, H. Sun, Large spot diameter nanosecond laser treatment of aluminum alloy sheets for high-speed superhydrophobic hierarchical micro- and nanostructured surface preparation, Surf. Coat. Technol. 361 (2019) 249–254, https://doi.org/10.1016/j.surfcoat.2019.01.020.
[21] L.Y. Mei, J. Sun, Y. Li, Y.Y. Lei, X.D. Du, Y.C. Wu, Fabrication of composite modified layer on aluminium alloy by surface mechanical nano-alloying combined with nitriding, Appl. Surf. Sci. 499 (2020) 143915, https://doi.org/10.1016/j.apsusc.2019.143915.
[22] M. Carvalho da Cunha, M.S. Fernandes de Lima, The influence of laser surface treatment on the fatigue crack growth of AA 2024-T3 aluminum alloy alclad sheet, Surf. Coat. Technol. 329 (2017) 244–249, https://doi.org/10.1016/j.surfcoat.2017.08.052.
[23] I.B. Okipnyi, P.O. Maruschak, V.I. Zakiev, V.S. Mocharskyi, Fracture mechanism analysis of the heat-resistant steel 15Kh2MFA(II) after laser shock-wave processing, J Fail. Anal. Prev. 14 (2014) 668–674, https://doi.org/10.1007/s11668-014-9869-4.
[24] Z. Qin, D.-H. Xia, Y. Zhang, Z. Wu, L. Liu, Y. Lv, Y. Liu, W. Hu, Microstructure modification and improving corrosion resistance of laser surface quenched nickel–aluminum bronze alloy, Corros. Sci. 174 (2020) 108744, https://doi.org/10.1016/j.corsci.2020.108744.
[25] C. Zhou, H. Li, G. Chen, G. Wang, Z. Shan, Effect of single pulsed picosecond and 100 nanosecond laser cleaning on surface morphology and welding quality of aluminium alloy, Opt. Laser Technol. 127 (2020) 106197, https://doi.org/10.1016/j.optlastec.2020.106197.
[26] B. Dhakal, S. Swaroop, Effect of laser shock peening on mechanical and microstructural aspects of 6061-T6 aluminum alloy, J. Mater. Process. Technol. 282 (2020) 116640, https://doi.org/10.1016/j.jmatprotec.2020.116640.
[27] A.S. Sabau, H.M. Meyer III, D.N. Leonard, Laser-interference pulse number dependence of surface chemistry and sub-surface microstructure of AA2024-T3 alloy, Opt. Laser Technol. 131 (2020) 106457, https://doi.org/10.1016/j.optlastec.2020.106457.
[28] X. Li, B. Zhang, H. Wang, T. Yu, Control of the floating zone stability during electron beam melting process of Ni-25%Si alloy, J. Manuf. Processes 45 (2019) 702–709, https://doi.org/10.1016/j.jmapro.2019.08.008.
[29] R. Wang, J. Yu, D. Wei, C. Meng, Surface microstructures and improved mechanical property of 40CrMn steel induced by continuous scanning electron beam process, Nucl. Instr. Meth. Phys. Res., Sect. B 459 (2019) 130–136, https://doi.org/10.1016/j.nimb.2019.08.020.
[30] L. Wang, K. Wang, N. Erkan, Y. Yuan, J. Chen, B. Nie, F. Li, K. Okamoto, Metal material surface wettability increase induced by electron beam irradiation, Appl. Surf. Sci. 511 (2020) 145555, https://doi.org/10.1016/j.apsusc.2020.145555.
[31] H. Bian, K. Aoyagi, Y. Zhao, C. Maeda, T. Mouri, A. Chiba, Microstructure refinement for superior ductility of Al–Si alloy by electron beam melting, Addit. Manuf. 32 (2020) 100982, https://doi.org/10.1016/j.addma.2019.100982.
[32] Y. Hao, B. Gao, G.F. Tu, S.W. Li, C. Dong, Z.G. Zhang, Improved wear resistance of Al–15Si alloy with a high current pulsed electron beam treatment, Nucl. Instr. Meth. Phys. Res., Sect. B (2011) 1499–1505, https://doi.org/10.1016/j.nimb.2011.04.010.
[33] B. Gao, Y. Hao, W.F. Zhuang, G.F. Tu, W.X. Shi, S.W. Li, S.Z. Hao, C. Dong, M.C. Li, Study on continuous solid solution of Al and Si elements of a high current pulsed electron beam treated hypereutectic Al17.5Si alloy, Phys. Proc. 18 (2011) 187–192, https://doi.org/10.1016/j.phpro.2011.06.079.
[34] Y. Hao, B. Gao, G.F. Tu, H. Cao, S.Z. Hao, C. Dong, Surface modification of Al–12.6Si alloy by high current pulsed electron beam, Appl. Surf. Sci. 258 (2012) 2052–2056, https://doi.org/10.1016/j.apsusc.2011.04.104.
[35] D. Zaguliaev, V. Gromov, Y. Rubannikova, S. Konovalov, Y. Ivanov, D. Romanov, A. Semin, Structure and phase states modification of AL-11SI-2CU alloy processed by ion-plasma jet and pulsed electron beam, Surf. Coat. Technol. 383 (2020) 125246, https://doi.org/10.1016/j.surfcoat.2019.125246.
[36] S. Konovalov, D. Zaguliaev, Y. Ivanov, V. Gromov, A. Abaturova, Modification of Al-10Si-2Cu alloy surface by intensive pulsed electron beam, J. Mater. Res. Technol. 9 (2020) 5591–5598, https://doi.org/10.1016/j.jmrt.2020.03.083.
[37] J. An, X.X. Shen, Y. Lu, Y.B. Liu, R.G. Li, C.M. Chen, M.J. Zhang, Influence of high current pulsed electron beam treatment on the tribological properties of Al–Si–Pb alloy, Surf. Coat. Technol. 2 (2006), https://doi.org/10.1016/j.surfcoat.2005.07.106.
[38] J. Li, X. Cheng, Z. Li, X. Zong, X.-H. Chen, S.-Q. Zhang, H.-M. Wang, Microstructures and mechanical properties of laser additive manufactured Al-5Si-1Cu-Mg alloy with different layer thicknesses, J. Alloys Compd. 789 (2019) 15–24, https://doi.org/10.1016/j.jallcom.2019.03.101.
[39] J. Li, X. Cheng, Z. Li, X. Zong, S.-Q. Zhang, H.-M. Wang, Improving the mechanical properties of Al-5Si-1Cu-Mg aluminum alloy produced by laser additive manufacturing with post-process heat treatments, Mater. Sci. Eng., A 735 (2018) 408–417, https://doi.org/10.1016/j.msea.2018.08.074.
[40] D. Zaguliaev, S. Konovalov, Y. Ivanov, V. Gromov, Microstructure and micro-hardness behavior of Ti–Y_2O_3–Al–Si composite coatings prepared in electron-plasma alloying, Mater. Charact. 158 (2019), https://doi.org/10.1016/j.matchar.2019.109934.
[41] D.V. Zagulyaev, Y.F. Ivanov, A.M. Glezer, V.E. Gromov, S.V. Konovalov, Effect of the density of electron beam energy on the structure and mechanical characteristics of surface layers of hypoeutectic silumin, Bull. Russ. Acad. Sci. Phys. 83 (2019) 1282–1288, https://doi.org/10.3103/S106287381910023X.
[42] V. Sarychev, S. Nevskii, S. Konovalov, A. Granovskii, Y. Ivanov, V. Gromov, Model of nanostructure formation in Al-Si alloy at electron beam treatment, Mater. Res. Express. 6 (2019) 26540, https://doi.org/10.1088/2053-1591/aaec1f.